1   **Authors:** James R. Collins[1,2*†], Paul D. Fucile[3], Glenn McDonald[4], Justin E. Ossolinski[2], Richard G.

2   Keil[5], James R. Valdes[3], Scott C. Doney[2], and Benjamin A. S. Van Mooy[2*]

3   **Title:** An autonomous, *in situ* light-dark bottle device for determining community respiration and net

4   community production

5   **Affiliations:** [1] MIT/WHOI Joint Program in Oceanography/Applied Ocean Science and Engineering,

6   Woods Hole, Massachusetts, USA

7   [2] Department of Marine Chemistry and Geochemistry, Woods Hole Oceanographic Institution,

8   Woods Hole, Massachusetts, USA

9   [3] Department of Physical Oceanography, Woods Hole Oceanographic Institution, Woods Hole, MA

10   02543, USA

11   [4] Department of Applied Ocean Physics and Engineering, Woods Hole Oceanographic Institution,

12   Woods Hole, MA 02543, USA

13   [5] School of Oceanography, University of Washington, Seattle, WA 98195, USA

14   *** Correspondence:** James R. Collins, james.r.collins@aya.yale.edu or Benjamin A. S. Van Mooy,

15   bvanmooy@whoi.edu

16   **† Present Address:** James R. Collins, School of Oceanography and eScience Institute, University of

17   Washington, Seattle, WA 98195, USA

18   **Running head:** Autonomous observations of community metabolism

19   **Keywords:** respiration, community metabolism, aquatic microbial ecology, autonomous

20   instrumentation, optodes, dissolved oxygen, ocean observing

21

Abstract

We describe a new, autonomous, incubation-based instrument that is deployed *in situ* to determine rates of gross community respiration and net community production in marine and aquatic ecosystems. During deployments at a coastal pier and in the open ocean, the PHORCYS (*PHO*tosynthesis and *R*espiration *C*omparison-*Y*ielding *S*ystem) captured dissolved oxygen fluxes over hourly timescales that were missed by traditional methods. The instrument uses fluorescence-quenching optodes fitted into separate light and dark chambers; these are opened and closed with piston-like actuators, allowing the instrument to make multiple, independent rate estimates in the course of each deployment. Consistent with other studies in which methods purporting to measure the same metabolic processes have yielded divergent results, respiration rate estimates from the PHORCYS were systematically higher than those calculated for the same waters using a traditional two-point Winkler titration technique. However, PHORCYS estimates of gross respiration agreed generally with separate incubations in bottles fitted with optode sensor spots. An Appendix describes a new method for estimating uncertainties in metabolic rates calculated from continuous dissolved oxygen data. Multiple successful, unattended deployments of the PHORCYS represent a small step toward fully autonomous observations of community metabolism. Yet the persistence of unexplained disagreements among aquatic metabolic rate estimates — such as those we observed between rates calculated with the PHORCYS and two existing, widely-accepted bottle-based methods — suggests that a new community intercalibration effort is warranted to address lingering sources of error in these critical measurements.

Introduction

Accurate, reproducible, and cost-effective estimates of aerobic respiration and primary production in aquatic systems are essential for research across a diverse array of disciplines in the environmental sciences (del Giorgio and Williams, 2005; Volkmar and Dahlgren, 2006; Staehr et al., 2012). Rate measurements of these two metabolic parameters can be applied to various problems, including validating the biogeochemical components of global climate models (Denman et al., 2007), determining the trophic status of surface-water planktonic communities in open ocean ecosystems (Williams, 1998), measuring rates of biological oxygen demand (BOD) in treated wastewater (Spanjers et al., 1994), and identifying unexpected metabolisms in the deep ocean (Reinthaler et al., 2010).

While an increasing demand for metabolic rate data has encouraged the development of many different methods for estimating rates of photosynthesis (Ducklow and Doney, 2013), the number of new methods for measuring aerobic respiration at the community scale has lagged behind considerably (del Giorgio and Williams, 2005). The majority of field-based methods for measuring rates of respiration and primary production in the ocean fall largely into two categories: (1) *in situ* geochemical tracer techniques that track changes in the concentration or isotopic composition of dissolved oxygen and carbon dioxide within ocean water masses (e.g., the surface mixed layer), and (2) *in vitro* incubation techniques that track the rates at which plankton exchange oxygen or carbon dioxide in discrete seawater samples (i.e., bottle incubations). The merits and faults of these two categories of approaches have been vigorously debated while significant and often unexplained differences are noted in the rate estimates they yield (Duarte et al., 2013; Ducklow and Doney, 2013; Williams et al., 2013). The former category has benefited considerably from recent advances in optical sensor technology (Moore et al., 2009), mass spectrometry (Goldman et al., 2015), and techniques for analysis of optical sensor data from autonomous underwater vehicles (Nicholson et al.,

68   2015). By maximizing the extent to which sensors are integrated into the surrounding environment,

69   low-power instruments increase the spatial and temporal resolution of geochemical tracers *in situ* and

70   permit increasingly autonomous, long-term deployments (Prien, 2007; Riser and Johnson, 2008;

71   Porter et al., 2009).

72   By contrast, the field has seen relatively few technical advances in *in vitro* incubation

73   techniques. *In vitro* techniques provide an important complement to *in situ* methods because they are

74   sensitive to short-term perturbations and are amenable to experimental design. For these reasons, the

75   traditional two-point light and dark bottle incubation technique (Gaarder and Gran, 1927) and the ^{14}C

76   incubation method (Steeman Nielsen, 1952) continue to dominate incubation-based studies, although

77   a number of other methods based on electron transport (e.g., Kenner and Ahmed, 1975) or fluxes of

78   ^{18}O or CO_2 (Bender et al., 1987; Robinson and Williams, 2005) have been introduced over the course

79   of the last half-century. A number of these methods have been incorporated into modern designs for

80   benthic flux chambers and so-called "benthic landers," enabling investigators to capture fluxes of

81   oxygen and other gases *in situ* at the sediment-water interface instead of in core samples aboard ship

82   (Hammond et al., 2004; compare, e.g., Martens et al., 2016, Fuchsman et al., 2015, or Lee et al.,

83   2015, to Kim et al., 2015). However, even the most advanced of these devices can require the use of

84   divers or remotely operated vehicles (ROVs) for deployment, maintenance, or recovery.

85   Additionally, by their nature, few of these designs can be programmed to conduct multiple

86   incubations over the course of a single deployment. Taylor et al. addressed this obstacle with the

87   submersible incubation device (SID), which for the first time allowed multiple, unattended

88   incubations with ^{14}C-bicarbonate to be conducted *in situ* (Taylor and Doherty, 1990; Taylor et al.,

89   1993). The SID represented a significant advance but was limited by its relatively small 400 mL

90   incubation chamber and its reliance on the use of radiolabeled reagents.

91   Among the advances most consequential for *in situ* instrumentation was the adaptation to

92   marine applications of optical technologies such as optodes (e.g., Klimant et al., 1995; Tengberg et

93   al., 2006) and optode sensor spots (e.g., Warkentin et al., 2007), which exploit fluorescence

94   (luminescence) quenching to measure dissolved oxygen concentrations non-destructively and without

95   themselves contributing to oxygen consumption in the sample. Integral optodes and sensor spots

96   based on the same technology have now been successfully used in a variety of shipboard

97   configurations to measure rates of gross community respiration in whole, unconcentrated and

98   unfiltered water samples and in water containing particle material from marine and aquatic

99   environments (Edwards et al., 2011; Wikner et al., 2013; Collins et al., 2015). More recently,

100   shipboard *in vitro* measurements of respiration within individual marine particles were made

101   successfully using oxygen microelectrodes (Belcher et al., 2016a; Belcher et al., 2016b). A

102   significant recent advance was also achieved with the RESPIRE device, which uses an optode fitted

103   into a modified sediment trap to make particle respiration measurements *in situ* (Boyd et al., 2015;

104   McDonnell et al., 2015).

105   Despite the significant progress represented in these optode-driven systems, incubation-based

106   methods remain prone to a number of sources of error that demand reconciliation. These can be

107   generally divided into two categories: (1) those that result from the preparation for or act of

108   incubating natural microbial populations and (2) errors inherent in the method used to determine the

109   concentration of dissolved oxygen (e.g., Winkler titration, fluorescence-quenching optode, or Clark

110   electrode). The sources of uncertainty associated with bottle/chamber incubations span both

111   categories and include (1) contamination, disruption, or bias introduced through the process of

112   obtaining seawater samples from depth and preparing them for incubation (Suter et al., 2016;

113   Tamburini et al., 2013); (2) unrepresentative incubation conditions that do not faithfully reproduce

114   the variations in temperature, turbulence, and light inherent in natural systems; (3) so-called "bottle

115   effects" associated with low-volume incubations which may limit nutrient availability (Furnas, 2002)

116   or induce unnatural changes in community structure (Venrick et al., 1977; Calvo-Díaz et al., 2011);

117   and (4), in the case of metabolic rate measurements extrapolated from Winker (1888) titrations, the

118   lack of temporal resolution inherent in measurements based only on two endpoints. In any study

119   where incubations are used, the choice of incubation methodology places inherent limits on the

120   spatial and temporal resolution of the data collected (Karl et al., 2001). The integration of point

121   measurements — data sparse in time and/or space, whether based on *in situ* observations or

122   incubations — also creates significant representation error. One solution to this problem is to greatly

123   increase the number of measurements made during data collection using automated technologies.

124   We describe here the *PHO*tosynthesis and *R*espiration *C*omparison-*Y*ielding *S*ystem

125   (PHORCYS), a large-volume (i.e., > 2.5 L), light and dark chamber incubation system for

126   autonomous measurement of rates of primary production and respiration at high temporal resolution

127   and under *in situ* conditions. In designing the instrument, we endeavored to minimize the major

128   hypothesized sources of uncertainty associated with traditional incubation-based methods while

129   constructing a system that functions autonomously and interrogates water samples non-destructively.

130   We also sought to eliminate or reduce the need for repeated wet-chemical field measurements such as

131   Winkler oxygen titrations or reagent-based methods used in other autonomous systems. We first

132   describe design and validation of the PHORCYS using two independent methods, and then present

133   results of several deployments of the instrument in different ecosystem types.

134   **Materials and procedures**

135   *Instrument design and operation*

136   The PHORCYS is composed of only a few basic components, making the design highly

137   scalable and cost-effective (Fig. 1a,b). In nearly all instances, "off the shelf" components of different

138   size or capacity can be easily substituted for those we describe here. The PHORCYS consists of two

139   polycarbonate plastic chambers (usable vol. 5.7 L; Table 1), several auxiliary sensors for collection

140   of environmental data in the ambient water mass outside the chambers, and a watertight power

141   supply, control, and data recording module (Fig. 1a). A piston-like, magnetically coupled actuator is

142   programmed to open and close each chamber at a specified interval, allowing users to perform

143   multiple, unattended incubations over the course of a single deployment. The chamber seals are

144   tapered to avoid the use of rubber O-rings that might have introduced a source of organic

145   contamination into the sample water. In experiments, the polycarbonate plastic used for the

146   PHORCYS incubation chambers reduced photosynthetically active radiation (PAR) within the

147   transparent chamber to 83% of incident strength; we present a means of accounting for this

148   attenuation, below. The opaque chamber was darkened by application of a coating to the outside of

149   the cylinder. All PHORCYS components are mounted to a stainless-steel frame, allowing the

150   instrument to operate to a depth of 100 m.

151   Dissolved oxygen concentrations in the two chambers are monitored with fast-response,

152   fluorescence quenching oxygen optodes (Aanderaa model 4531D; accuracy < 8 μM O_2; resolution <

153   1 μM O_2; response time < 30 s; Aanderaa Data Instruments, Inc., Bergen, Norway); each optode is

154   fitted into its chamber using a water- and gas-tight flange assembly. The instrument also has several

155   external sensors, including a third optode to monitor dissolved oxygen concentrations in the water

156   mass outside of the two chambers, PAR sensor, beam transmissometer, chlorophyll fluorometer, and

157   CTD. We did not investigate whether the arrangement of these sensors had any effect on the external

158   dissolved oxygen field surrounding the instrument.

159   With a full sensor suite, the nominal power consumption of the PHORCYS is 50 mA at 12V;

160   standby current is 2 mA. When programmed to sample at a 50 % duty cycle, a single 12V primary

161   'D' cell battery pack (20,000 mAh capacity) will power the instrument for up to 30 d in an

7

162 unattended deployment mode. Data are recorded in an ASCII fixed-field format onto a micro SD card

163 in a DOS-readable format. For attended deployments, a combination communications and external

164 power port provides the ability to observe data in real time, allow program updates, download data,

165 and power the instrument indefinitely. The sampling interval is nominally set to 1 min, though data

166 can be collected as frequently as every 15 s. The acquisition program determines sampling activity by

167 way of a real-time clock. The chambers can thus be programmed to open and close at any time,

168 allowing the investigator to make multiple incubations of any desired length. In the configuration

169 used to acquire the data presented here, (Fig. 2, ◻ symbol; e.g., Fig. 3) the chambers were

170 programmed to open at or around sunrise and the same operation was repeated at sunset, providing

171 two incubations in each 24 h period that aligned with the beginning and end of the photoperiod. The

172 chambers are opened and then closed sequentially (i.e., one after the other) to reduce total current

173 draw from the power source. The chambers remain open for 30 min at the outset of each incubation,

174 providing sufficient time for the water to be fully exchanged before closure; we confirmed this

175 flushing time was sufficient in both quiescent and flowing (~ 1 m s^{-1}) waters using a series of tests

176 with a tracer dye (results not shown). While we used a standard 30 min flush time in the deployments

177 for which data is presented below, any time can be specified in the instrument's control software,

178 which is written in BASIC.

179   The earlier PHORCYS data from 2012 (Fig. 2, ⬤ symbols; e.g., Fig. 4) were obtained using a

180 prototype instrument that permitted only one incubation cycle per deployment. This prototype (Fig.

181 1b) was assembled from two 2.5 L Niskin-style sampling bottles mounted to an aluminum frame

182 (opaque polyvinylchloride and transparent polycarbonate plastic, respectively; actual usable volume,

183 2.6 L; General Oceanics, Inc., Miami, FL, USA). Closure of the chambers for incubation was

184 effected using an electrolytic time release (i.e., "burn wire") system. Prior to deployment, the Niskin

185 bottle endcaps were cocked open and the retaining cable was rigged to a fusible burn wire plug. Once

186   in the water, a sufficient current was applied to the burn wire at a time set by the user, corroding the

187   wire and allowing the bottle endcaps to close. The chambers were then sealed and the incubation

188   began. For the deployments presented here, we programmed the chambers to close approximately 45

189   min after the PHORCYS had reached the desired depth. In the prototype instrument, Aanderaa model

190   4330F optodes (accuracy < 8 µM O_2; resolution < 1 µM O_2) were used to record dissolved oxygen

191   concentrations.

192   *Instrument deployments*

193   We conducted 6 unattended deployments of the PHORCYS in 3 distinct ecosystem types in

194   the North Atlantic basin (Fig. 2; Table 2; Supplemental Table 1). Open-ocean deployments (2 to 7 d

195   in length, using the prototype instrument) were conducted during cruises aboard the R/V *Knorr*;

196   during these deployments, the instrument was suspended at various depths in the euphotic zone from

197   a drifting surface buoy (Fig. 1c). Deployment and recovery were accomplished in 45-60 min from a

198   standard oceanographic research platform (Supplemental Fig. 1). An Argo satellite beacon (Fig. 1c)

199   allowed us to track the array remotely between deployment and recovery while the ship traveled up

200   to 300 km away to conduct other shipboard scientific operations; we specifically designed both

201   models of the PHORCYS to be wholly autonomous, incurring a minimal burden on other shipboard

202   operations. Pierside deployments were conducted using the present, multiple-incubation version of

203   the PHORCYS at the Iselin Marine Facility, Woods Hole, MA, USA (41º 31' 24" N 70º 40' 20" W);

204   the site adjoins a highly productive coastal embayment. In both cases, oxygen concentrations (µmol

205   L^{-1} O_2), percent saturation, and temperature were then recorded for each chamber at 1 min intervals.

206   Post-acquisition corrections for salinity were applied to both the open-ocean and coastal data using

207   concurrent observations of salinity and manufacturer-supplied correction coefficients. Concurrent

208   salinity data were obtained from the continuous, flow-through CTD system aboard the R/V *Knorr*

209   (for open-ocean deployments) or from the Seabird CTD unit mounted as an external sensor on the

210   present PHORCYS model (2016 coastal deployments). Due to the limited number of at-sea

211   deployments of the PHORCYS prototype and the challenges we encountered during our initial

212   cruises, we pooled our prototype results with the data we later obtained from the production-model

213   instrument in order to assemble a larger, more robust dataset for subsequent analysis.

214   *Instrument calibration and choice of deployment depth*

215   Optodes were calibrated before each pierside deployment and prior to each research cruise

216   using a two-point method, assuming a linear response between end-members. An air-saturated

217   solution was obtained according to manufacturer instructions by bubbling ambient air for approx. 30

218   min through a sufficient volume of Milli-Q water using an aquarium stone; a zero-oxygen solution

219   was obtained by dissolving an excess of reagent-grade sodium sulfite into a beaker containing Milli-

220   Q water. The optodes were then calibrated at atmospheric temperature and pressure, as recommended

221   by the manufacturer. At the open-ocean stations, we deployed the prototype instrument within the

222   euphotic zone at depths where the observed flux of photosynthetically active radiation (PAR;

223   wavelengths 400-700 nm) was between 10-30% of the incident flux at the surface. The depth of the

224   euphotic zone (z_{eu}, defined as the depth at which PAR = 1 % of incident intensity) was identified

225   using profiles from shipboard hydrocasts. At each of these stations, we calculated an equivalent

226   deployment depth (z_{equiv}) that accounted for light attenuation by the transparent chamber's

227   polycarbonate plastic, according to a modification of the standard equation for the exponential decay

228   of light with depth:

229     $$I_z(PAR) = \frac{I_0(PAR)e^{-K_d(PAR)z_{equiv}}}{T(PAR)} \qquad (1)$$

230   where $I_0(PAR)$ and $I_z(PAR)$ are, respectively, the incident PAR intensity and intensity at depth z,

231     $K_d(PAR)$ is the diffuse attenuation coefficient for the PAR spectral band (calculated from the

232   hydrocast profile at each station), and $T(PAR)$ is the transmissivity of the polycarbonate plastic

233   expressed as a fraction (0.83). Pierside deployments of the present PHORCYS model were conducted

234   at a depth of 1.5 m.

235   *Instrument validation by two independent methods*

236   First, to validate the optodes' ability to accurately track respiration, we used a standard

237   analytical method — two-point Winkler titration — to determine dissolved oxygen consumption in

238   triplicate water samples at the beginning and end of each incubation period (present model

239   instrument) or deployment (for data obtained with the prototype). Winkler titrations were conducted

240   in 125 mL BOD bottles according to EPA Method 360.2 as modified for shipboard determination in

241   seawater (Knapp et al., 1989). Initial Winkler titrations were made in samples collected within 15

242   min of deployment using a Niskin or Go-Flo bottle suspended at the same depth as the instrument. A

243   set of three darkened 125 mL BOD bottles containing water from the same Niskin or Go-Flo bottle

244   was incubated at *in situ* temperature until the PHORCYS was recovered or the incubation period

245   ended; these samples were then sacrificed according to the same protocol. The BOD bottles used in

246   these incubations were triple-rinsed with 10 % HCl and then Milli-Q water prior to sampling. All

247   reagents for Winkler titrations were A.C.S. grade or better; the sodium thiosulfate titrant was

248   standardized daily. Amperometric titration was performed using an autotitrator (Metrohm 904

249   Titrando; Metrohm USA, Inc., Riverview, FL).
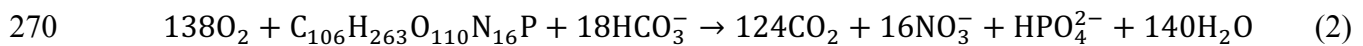
250   As an additional means of comparison during the open-ocean deployments, we also tracked

251   changes in dissolved oxygen in a series of continuously monitored shipboard bottle incubations.

252   Water from the PHORCYS deployment depth was retrieved for these incubations from a hydrocast

253   made within 1 h of deployment. Incubations were conducted in gas-tight, 300 mL glass BOD bottles;

254   at least 5 replicates were used for each series of measurements. Determination of dissolved oxygen

255 was made at 3 to 9 h intervals using optode spot minisensors (PreSens PSt3; response time < 40 s;

256 Precision Sensing GmbH, Regensburg, Germany; Warkentin et al., 2007) that were glued to the

257 inside surfaces of the bottles using food-quality silicone cement. The use of these optode spots

258 eliminated the need for drawing of aliquots from the sample bottles; the bottles had been soaked in

259 Milli-Q water for > 2 months following application of the sensor spots. Incubations were conducted

260 in the dark at *in situ* temperature as described in Edwards et al. (2011).
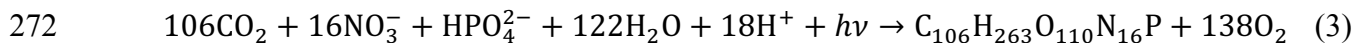
261 *Data analysis*

262 *PHORCYS rate calculations*

263   Volumetric rates of gross community respiration (GR) and net community production (NCP)

264 were calculated by linear least-squares regression of observations of dissolved oxygen concentration

265 over the length of the deployment (prototype model) or incubation period (present model). We

266 assumed the only significant chemical reactions contributing to oxygen consumption and evolution in

267 the two chambers were aerobic respiration and photosynthesis. For organic matter of elemental

268 stoichiometry roughly corresponding to that of Redfield (1934) and assuming production is based on

269 nitrate, these redox reactions can be represented as (after Stumm and Morgan, 2013):

270      $$138O_2 + C_{106}H_{263}O_{110}N_{16}P + 18HCO_3^- \rightarrow 124CO_2 + 16NO_3^- + HPO_4^{2-} + 140H_2O \quad (2)$$

271 and

272      $$106CO_2 + 16NO_3^- + HPO_4^{2-} + 122H_2O + 18H^+ + h\nu \rightarrow C_{106}H_{263}O_{110}N_{16}P + 138O_2 \quad (3)$$

273 As is the case with the classic light and dark bottle incubation technique, we assumed that only

274 respiration was taking place in the dark (i.e., GR; reported as positive quantities), while both

275 reactions were taking place simultaneously in the presence of light (i.e. NCP; in reality,

12

276   photorespiration also contributes to oxygen consumption in the light bottle). Finally, where possible,

277   we estimated the rate of gross primary productivity (GPP) according to the relationship

278   $$GPP = NCP + GR \qquad (4)$$

279   To estimate uncertainties in PHORCYS rate estimates, we adapted an effective degrees of freedom

280   technique traditionally applied to time-series data in physical oceanography (Emery and Thomson,

281   2001). The method, which serves as an alternative to the standard error of the regression slope in

282   instances when true replication cannot be achieved, is described in detail in the Appendix.

283   *Rate calculations from Winkler titration samples and sensor spot incubations*

284   For the Winkler titration samples, GR was calculated using a difference of means,

285   $$GR = -\frac{dO_2}{dt} \qquad (5)$$

286   where dO_2 is the difference between the mean dissolved oxygen concentration in samples sacrificed

287   at the final incubation timepoint and the mean measured at the initial timepoint and dt is the

288   incubation duration. For the sensor spot incubations, we calculated rates for each bottle using a linear

289   least-squares regression of all observations recorded over the time period; we then averaged the rates

290   obtained for the various replicates to obtain a final estimate. Uncertainties in rates based on the

291   Winkler titration method were determined from the standard deviations of the dissolved oxygen

292   concentrations measured in the replicates at each timepoint. For rates based on the sensor spot

293   incubations, we used the standard error of regression. While we report metabolic rate estimates from

294   the PHORCYS in oxygen-based units, a stoichiometric relationship such as the molar respiratory

295   quotient of Anderson and Sarmiento (1994) can be applied to convert these estimates to units of

296   carbon.

13

Assessment

PHORCYS metabolic rate estimates

299   We observed a significant degree of daily and hourly variability in the time series data from

300   each PHORCYS deployment (e.g., Fig. 3 and 4). This variability manifested itself in a wide range of

301   metabolic rate estimates (Table 2; Supplemental Table 1) that reflect the interaction of multiple

302   biological and physical forcings, including diel changes in cellular growth cycle, surface-layer water

303   temperature, and irradiance. Daily rates of GR were estimated from dark chamber data for all

304   PHORCYS deployments (Table 2). For data obtained with the present model instrument, hourly rates

305   were calculated for each incubation segment (Fig. 3); these were extrapolated to daily rates to

306   facilitate comparison with other studies and with data from the prototype instrument. For open-ocean

307   data obtained with the PHORCYS prototype, daily rates were calculated using the entire DO time

308   series from each deployment. Erroneous readings from one of the optodes and a system malfunction

309   prevented us from recovering usable NCP data from the transparent chamber during two of the open-

310   ocean deployments of the prototype instrument. During the 24-27 April 2012 deployment, the chosen

311   depth of 29 m provided insufficient PAR (< 3% of surface intensity) to support measurable

312   photosynthesis in the transparent chamber; consequently, we could not calculate NCP or GPP for this

313   station (Supplemental Table 1). An obstruction prevented the transparent chamber from closing

314   during the November 2016 deployment, allowing us to recover useful data from only the dark

315   chamber.

316   We captured daily rates of GR ranging from 1.8 ± 0.2 μmol O_2 L^{-1} d^{-1} at a mid-latitude

317   station in the North Atlantic to 10.5 ± 7.5 and 18.9 ± 1.9 μmol O_2 L^{-1} d^{-1} in two different water

318   masses at the Woods Hole pier in early November (Fig. 3 and 4; Table 2). The wide variation in GR

319   we observed with the PHORCYS covers a significant range of the rates for marine systems compiled

320   by Robinson and Williams (2005). Daily rates of GPP at the PHORCYS deployment depth ranged

321   from essentially zero on several days at a mid-latitude station in the North Atlantic (Supplemental

322   Table 1) to 3.6 ± 0.5 µmol O_2 L^{-1} d^{-1} during a coccolithophore bloom (Collins et al., 2015) in the

323   sub-Arctic North Atlantic (Fig. 4). Rates of NCP at the deployment depth ranged from -2.0 ± 0.4

324   µmol O_2 L^{-1} d^{-1} to -4.2 ± 0.2 µmol O_2 L^{-1} d^{-1} (Supplemental Table 1).

325   **Discussion**

326   *Subdaily variation in rates of metabolism; choices concerning data analysis*

327   Increasing evidence suggests the significant sub- and inter-daily variation in metabolic

328   activity captured by the PHORCYS exists in almost all natural aquatic systems (Caffrey, 2004;

329   Staehr et al., 2012; Collins et al., 2013); even in oligotrophic waters, respiration and production rates

330   may change significantly from one day (or hour) to the next, even as the system maintains an overall

331   state of near trophic balance (Aranguren-Gassis et al., 2012). The types of fluctuations we observed

332   in the various dissolved oxygen time series obtained from the PHORCYS appear to be characteristic

333   of incubation-based *in situ* instruments. McDonnell et al. (2015) and Boyd et al. (2015) both

334   observed similar patterns in dissolved oxygen data during recent deployments of an *in situ* device

335   that measures oxygen consumption rates on marine particles.

336   Nevertheless, the subtle changes in DO concentration we observed in multi-day incubations

337   with the PHORCYS prototype (e.g., Fig. 4) suggest that a single regression line — fitted, in this case,

338   to align with the closing and opening of the chambers — might have been poorly suited to a time

339   series exhibiting such variation. While one might instead have divided the full time series into shorter

340   segments to compute several different regressions (e.g, according to the photoperiod), we chose to

341   define the interval for rate calculations from the prototype instrument according the chamber opening

342   and closing times. This allowed us to avoid the bias inherent in dividing such a time series into

343   smaller segments. The present PHORCYS model allows users to predefine multiple, shorter

344   incubation periods of length appropriate to the ecosystem (e.g., Fig. 3); this feature eliminates the

345   need for a choice between either a subjective, *ex post facto* division of data or the application of a

346   single regression that might fail to capture the observed variation.

347   *Evaluation of instrument performance using independent methods*

348   PHORCYS estimates of community respiration were systematically higher than those

349   calculated for the same waters using the two-point Winkler titration method (Fig. 5a; Table 2). While

350   there was a significant correlation between estimates from the two different methods ($r^2 = 0.42$; $p =$

351   0.04), the traditional Winkler titration approach appeared to underestimate rates of respiration by

352   nearly one-third. Alternatively, the PHORCYS could have overestimated true rates of respiration

353   through artificial stimulation of the microbial community or inadvertent retention of residual

354   dissolved oxygen by the chambers or optode. In contrast, rate estimates from the PHORCYS

355   generally agreed with those based on our non-destructive optode sensor spot incubations, though we

356   had only five data points on which to evaluate the correlation (Fig. 5b; correlation was not

357   statistically significant).

358   Wikner et al. (2013) observed close agreement (~ 3 % deviation) between gross community

359   respiration rates derived from continuous optode measurements in a shipboard incubation chamber (1

360   L, clear glass) and a series of parallel incubations based on a Winkler method in 120 mL glass BOD

361   bottles. In previous work, we observed similar coherence between rates derived from a two-point

362   Winkler method in 300 mL glass BOD bottles and those based on incubations in 125 mL glass BOD

363   bottles fitted with optode sensor spots (surface area : volume ratios as reported in Table 1; Collins et

364   al., 2015). Underlying the agreement among methods in these previous studies is a common reliance

365   on incubations aboard ship. One might therefore conclude that the observed divergence between

366   estimates of respiration from the PHORCYS and those we made with the Winkler titration method

367   are due to inherent differences between the *in situ* PHORCYS approach and shipboard incubation

368   methods. However, evidence suggests that use of the same method is not even a guarantor of

369   agreement. For example, Robinson et al. (2009) found that vastly different rates were obtained from

370   the same method of measuring primary production when the only the timescale of incubation was

371   varied.

372   *Possible sources of observed discrepancies between methods*

373   *Gas permeability of materials*

374   The materials chosen for construction of the PHORCYS, particularly the polycarbonate

375   plastic we used for the incubation chambers, represent one possible source of bias in our method. We

376   chose polycarbonate material for its durability, low cost, and, compared with other plastics such as

377   polyvinylchloride, minimal biological reactivity. Polycarbonate was selected for its minimal

378   biological reactivity in construction of at least two similar *in situ* incubation devices (Langdon et al.,

379   1995; Robert, 2012). However, polycarbonate, like most plastics, is at least partially permeable to

380   dissolved oxygen; by comparison, the borosilicate glass of which BOD bottles are fabricated is

381   nearly impermeable (Kjeldsen, 1993; Robert, 2012). While some diffusion of dissolved oxygen

382   across the polycarbonate chamber walls could have occurred during incubations with the PHORCYS,

383   thus biasing our results, we believe the effect would likely have been very modest given the

384   dissolved oxygen gradients and timescales typical of our deployments. First, the gradient necessary

385   to drive any diffusion across the PHORCYS chamber wall (i.e., the difference between the internal

386   and external dissolved oxygen concentrations) did not exceed 25 μmol O_2 L^{-1} during any

387   deployment; in the deployment presented in Fig. 3, the average difference between internal and

388   external concentrations was just 6.1 μmol O_2 L^{-1}. In a series of oxygen-diffusion experiments with a

389   device similar to the PHORCYS, Robert (2012) monitored the dissolved oxygen concentration inside

390   a polycarbonate chamber after the water inside was treated with sodium hydrosulfite to render it

391   anoxic. After manipulating the dissolved oxygen concentration in water outside the chamber to create

392   cross-boundary gradients ranging from approx. 50 µmol O_2 L^{-1} to > 350 µmol O_2 L^{-1}, the authors

393   observed little change in the dissolved oxygen concentration inside the chamber on timescales similar

394   to those of the PHORCYS deployments (11-12 h for the current version of the instrument; 3-5 d for

395   the PHORCYS prototype). Further, in a comprehensive study of the permeabilities of several gases

396   (O_2, N_2, CO_2, and CH_4) in various polymers, Kjeldsen (1993) concluded that bias introduced by

397   permeability should be taken into account primarily when certain materials such as silicone rubber

398   were considered for use in anoxic waters; silicone rubber is more than 250 times as permeable to

399   dissolved oxygen than the polycarbonate plastic we used in construction of the PHORCYS (Kjeldsen,

400   1993).

401   *Handling or sampling bias*

402   Errors or bias introduced during the handling and manipulation of samples for bottle

403   incubations might also explain some of the discrepancy in rate measurements. For example, the

404   PHORCYS minimizes physical disturbances associated with seawater handling: Since the instrument

405   takes seawater samples and then incubates them in place, the planktonic community is not subjected

406   to rapid changes in temperature, pressure, and light associated with bringing water samples to the

407   surface via hydrocast and preparing them for shipboard incubations (Calvo-Díaz et al., 2011). The

408   PHORCYS also minimizes another potential bias that can arise when water containing marine

409   microbes is sampled from Niskin bottles; Suter et al. (2016) found that variation in settling rates

410   among marine particles can lead to an undersampling of microbial communities on faster-sinking

411   particles, which can fall below the bottles' spouts before aliquots can be drawn.

412   *Biofouling and surface colonization*

413   While we did not observe any significant biofouling of the PHORCYS or its components

414   during the deployments for which data are presented here, unwanted biological growth represents a

415   significant challenge and source of potential bias when autonomous sensors are deployed in the

416   surface and mesopelagic ocean (Delauney et al., 2010; Manov et al., 2004; e.g., Collins et al., 2013).

417   We imagine biofouling could represent a significant obstacle during future deployments if the

418   deployment duration were to exceed 5-7 d (the maximum explored in this work; Table 2), or if the

419   instrument were deployed in a productive ecosystem during a period of elevated primary production.

420   Compare, however, Robert (2012), who reported little biofilm growth on the chamber of a similar

421   incubation-based instrument after deploying it with no fouling controls for several months in the

422   Mediterranean Sea.

423   The lack of visual evidence of fouling in the PHORCYS chambers notwithstanding, there is

424   substantial evidence that microbial colonization of surfaces happens rapidly in the marine

425   environment (Salta et al., 2013; Dang and Lovell, 2016). It is therefore almost certain that at least

426   some microbial colonization of the chamber walls would have taken place within the 3-5 d timescale

427   of our deployments. Because we did not make measurements of biofilm activity or species

428   abundance, it is impossible to diagnose what contribution these communities might have made to the

429   observed fluxes in dissolved oxygen. However, compared to the surface area to volume ratios of the

430   150 and 300 mL vessels in which the other rate measurements were made (125 mL bottle, 0.83; 300

431   mL bottle, 0.77), the lower surface area to volume ratios of the PHORCYS chambers (current model,

432   0.34; prototype, 0.67) provide fewer opportunities for colonization relative to the volume being

433   incubated (Table 1). There is also some evidence that the small volumes typical of BOD bottles may

434   induce non-representative changes in the planktonic microbial community during incubations on

435   timescales of 24-48 h (Pratt and Berkson, 1959); however, compare Fogg and Calvario-Martinez

436 (1989), who found that such bottle size effects were only significant during periods of very high

437 primary productivity. A thorough, systematic assessment of these so-called wall and bottle effects

438 should be part of the community intercalibration we advocate in our conclusion.

439 *Other possible sources of bias*

440   Alternatively, the well-documented dependence of community respiration rates on

441 temperature (Yvon-Durocher et al., 2012) might explain the apparent disagreement between methods.

442 While temperatures within the PHORCYS chambers fluctuated only according to the movement of

443 tidal water masses (Fig. 3) or the natural warming and cooling of the surface layer (Fig. 4), the

444 temperature inside the incubator in which the Winkler samples were kept during the shipboard

445 deployments fluctuated during each series of experiments by ± 2°C from the target. A further, more

446 intriguing explanation for the systematic discrepancy — pointing in this case to overestimation of

447 rates by the PHORCYS — is that dissolved oxygen could have accumulated on the optodes or inside

448 walls of the instrument chambers over the course of each deployment, in spite of the standard 30 min

449 flushing protocol. Wikner et al. (2013) offer convincing evidence for the accumulation of dissolved

450 oxygen on the optode surface and acrylic (polymethylmethacrylate) stopper used in their shipboard

451 incubation apparatus; the application of a correction factor for this bias reduced apparent rates

452 calculated from the optode time series relative to the Winkler method. We did not evaluate oxygen

453 retention by the polycarbonate plastic material of which the PHORCYS chambers were constructed.

454   The nature of linear regression itself may also play a role in differences observed between the

455 PHORCYS and the Winkler-based method. A least-squares regression line fit to a large set of

456 observations collected at high temporal frequency, such as those obtained from the PHORCYS, is

457 sensitive in some degree to each of those observations. In comparison, a rate calculated from the

458 beginning and ending oxygen concentrations in the two-point Winkler method is necessarily sensitive

459   only to those two observations; if some unrepresentative source of variability is present in just one

460   bottle, the entire measurement can be heavily biased. Regression of data from the PHORCYS thus

461   yields rate estimates which are robust to the sampling bias inherent in point measurements, yet the

462   technique leaves the underlying data intact to be further interrogated for information about natural

463   variability.

464   *The "deep breath" phenomenon*

465   Finally, while not evident in data from the deployments presented in Fig. 3 or 4, we did

466   occasionally observe a sharp initial decrease in dissolved oxygen concentration within the chambers

467   shortly after closure (data not shown). This phenomenon was reported extensively by Robert (2012)

468   during testing of a similar instrument in the Mediterranean Sea, and thus warrants further

469   investigation. The initial "deep breath" observed in these instances could reflect the rapid and

470   preferential utilization by the microbial community of a limited but highly labile fraction of the

471   dissolved organic carbon (DOC) pool within the chamber. Such a phenomenon has been observed

472   frequently in rates of DOC consumption in freshwater systems, where labile carbon is often

473   metabolized at a rapid rate in the initial minutes or hours of an incubation, leading to an apparent

474   decline in metabolic activity once the labile pool has been exhausted and the incubation progresses

475   (del Giorgio and Pace, 2008; Guillemette and del Giorgio, 2011; Guillemette, McCallister, et al.,

476   2013). While we did not directly observe a pronounced initial change in the rate of dissolved oxygen

477   consumption in any of our shipboard optode sensor spot incubations, it is possible that our sampling

478   interval (3 to 9 h; see above) was of insufficient resolution to detect it.

479   **Comments and recommendations**

480   Through autonomous collection of biogeochemical observations at uniquely high temporal

481   frequency, the PHORCYS yields estimates of community metabolic activity while simultaneously

482   freeing the analyst from the logistical constraints of attended water column sampling and preparation

483   of shipboard incubations. While we could not determine the origin of the systematic discrepancy

484   between the PHORCYS rate estimates and those based on the traditional two-point Winkler method,

485   the instrument's design allows investigators to avoid many of the potential biases associated with

486   bottle incubations that have been previously documented in the literature. The PHORCYS offers a

487   further advantage in that it can be used to collect information over multiple timescales about the

488   metabolic state of marine and aquatic ecosystems at minimal cost and burden to the user. While the

489   mixed-layer deployments we have presented here provided volumetric rates of ecosystem metabolism

490   at a single depth, multiple PHORCYS units could be deployed simultaneously at different depths in

491   the water column as a means of making depth-integrated rate measurements; one could compare

492   these rates to estimates obtained from *in situ* geochemical tracer studies. Future work could also

493   include direct, side-by-side comparison of metabolic rates obtained from the PHORCYS with those

494   from the classic, bottle-based ^{14}C or ^{13}C tracer methods.

495   In this spirit, we believe a new, community intercalibration effort is warranted to

496   systematically evaluate the many sources of uncertainty in incubation-based measurements of

497   community metabolism. The workshops of the Group for Aquatic Primary Productivity (GAP;

498   Figueroa et al., 2014) could serve as a model for such an effort, which should include comprehensive

499   evaluation of various combinations of incubation chamber materials, types of oxygen sensors,

500   chamber sizes, and incubation durations. Genetic and biogeochemical tools for characterizing the

501   extent, mechanisms, and effects of surface colonization within the incubation chambers would be

502   critical to the success of any such endeavor. We are optimistic such an effort might reveal the causes

503   of longstanding discrepancies such as those we observed between our PHORCYS rate estimates and

504   those we obtained with bottle-based methods.

505   **Acknowledgments**

520   **Availability of data and code**

521   A MATLAB script to read in, process, and estimate rates and uncertainties in dissolved

522   oxygen data from the PHORCYS is provided online at

523   https://github.com/jamesrco/DO_Instruments/. The script can be easily adapted to calculate N_{eff}-

524   based estimates of uncertainty in any dissolved oxygen time series. All PHORCYS and Winkler

525   titration data and other scripts required to reproduce the results and figures in this work are available

526   online in the same location.

527

23

Appendix

A new method for calculation of uncertainties in metabolic rate estimates

The ideal means of estimating uncertainties in PHORCYS rates would have been true biological replication, i.e., the simultaneous deployment of several identical instruments in the same water mass. One could then have used the standard deviation of the rate measurements in each different instrument as an estimate of the overall uncertainty. Because we had only one instrument — an exceedingly common situation in oceanographic work — such true replication was not possible. The standard error of the regression slope provides one possible estimate of uncertainty in time-series dissolved oxygen data; for example, this common approach was recently applied to data from *in situ* chamber incubations of sinking marine particle material (McDonnell et al., 2015). However, we assumed that the standard error of regression would significantly underestimate the true uncertainty in our estimates since it does take into account the reduced number of degrees of freedom in such a time series. Because the data points in such a dissolved oxygen time series are not independent of one another, there are almost always far fewer effective degrees of freedom N_{eff} in such data than the number of observations (i.e., data points) N (Emery and Thomson, 2001). (We represent the effective degrees of freedom by the notation N_{eff} in lieu of the N^* notation used by Emery and Thompson.)

Our approach was the following: For each time series of dissolved oxygen concentrations, we first approximated the integral time scale T of the data according to

$$T = \frac{1}{C(0)} \int_0^{B_0} C(\tau)\, d\tau \qquad \text{(A1)}$$

where $C(0)$ is the value of the autocorrelation function C of the time series at lag $\tau = 0$, and B_0 is the time lag of the autocorrelation function at the first zero crossing of the *x*-axis, which (after, e.g., Talley et al., 2011) we use as an estimate of the timescale of decorrelation. We then followed the

550 method of Emery and Thompson (2001) to estimate the effective number of degrees of freedom N_{eff}

551 from T, N, and Δt, where Δt is the sampling interval of the data:

$$N_{eff} = \frac{N\Delta t}{T} \quad (A2)$$

553 In this formulation, $N\Delta t$ is therefore the total length of the oxygen time series in which the rate

554 estimate was made. Finally, we used this N_{eff} to obtain $s_{\hat{\beta}_{1,adj}}$, an adjusted estimate of the

555 standardized uncertainty in the slope parameter of the regression (i.e., $\hat{\beta}_1$, the rate of dissolved

556 oxygen consumption or production), according to

$$s_{\hat{\beta}_{1,adj}} = \sqrt{\frac{SSE}{N_{eff}-2} \frac{N}{\Delta}} \quad (A3)$$

558 where SSE is the sum of the squared errors from the fit of the regression, i.e., $\sum_{i=1}^{N}(y_i - \hat{y}_i)^2$, N is

559 the number of observations (as above), and Δ is the determinant $NS_{xx} - S_x^2$. Eq. A3 is simply the

560 formula for calculation of the standard error of the regression slope in the unweighted case, except

561 that N_{eff} is used instead of N.

562   This method of estimating uncertainties in PHORCYS rates produced values of N_{eff}, the

563 number of effective degrees of freedom, which were typically $\ll N$, the number of observations in

564 the given dissolved oxygen time series (Table A1). Estimates of the integral time scale T ranged from

565 0.5 to 7.2 h; at station PS-2, the 77.4 h deployment for which data are presented in Fig. 4, we

566 estimated T to be 7.2 h (Table A1). Using the N_{eff} derived from these time scales, we obtained

567 adjusted uncertainty estimates for our PHORCYS rates ($s_{\hat{\beta}_{1,adj}}$) which were much greater in each

568 case than the standard error of the regression slope, $s_{\hat{\beta}_1}$ (compare mean precision of 24.8 % and 3.4

569 %, respectively; Table A1). While more robust than the corresponding $s_{\hat{\beta}_1}$, these $s_{\hat{\beta}_{1,adj}}$ still reflect a

570   fundamental limitation of linear regression: Both methods yield estimates of uncertainty which are

571   inversely proportional to the number of data points (i.e., the length of the underlying data series) and

572   the range of values spanned by the independent variable.

Figures
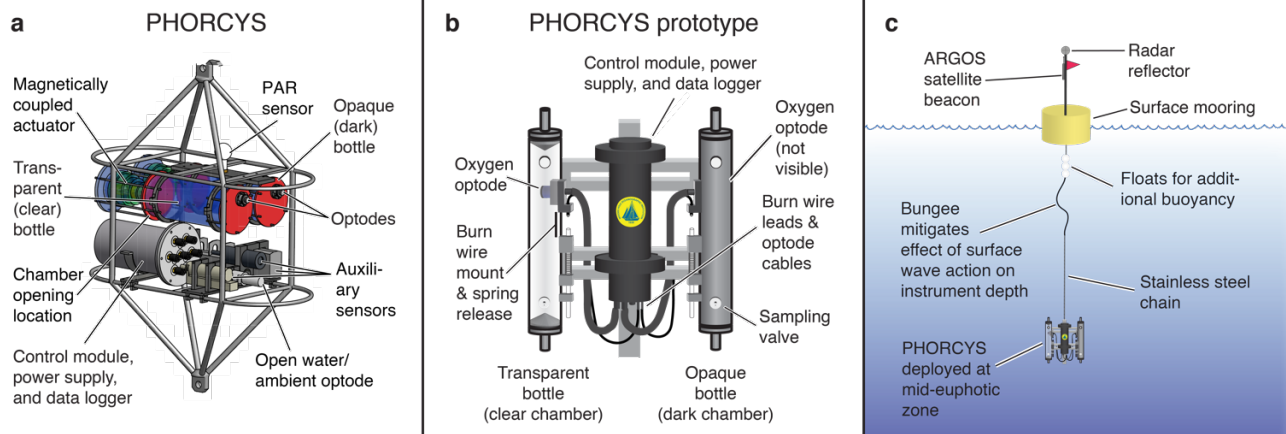
Fig. 1. Design and deployment of the PHORCYS. Major components of the current model

PHORCYS and prototype instrument are illustrated in (a) and (b), respectively. (a) The PHORCYS

uses magnetically-coupled actuators, allowing for multiple openings and closings of the chambers

during a single deployment. The current instrument also includes several sensors for collection of

auxiliary data in the water outside of the chamber, including photosynthetically active radiation

(PAR), conductivity, ambient temperature, transmissivity, and chlorophyll fluorescence. The

PHORCYS also includes a third optode to measure dissolved oxygen concentrations in the ambient

water mass outside of the two chambers. (c) Rigging scheme for open-ocean deployments from a

drifting surface mooring, as described in the text.

584
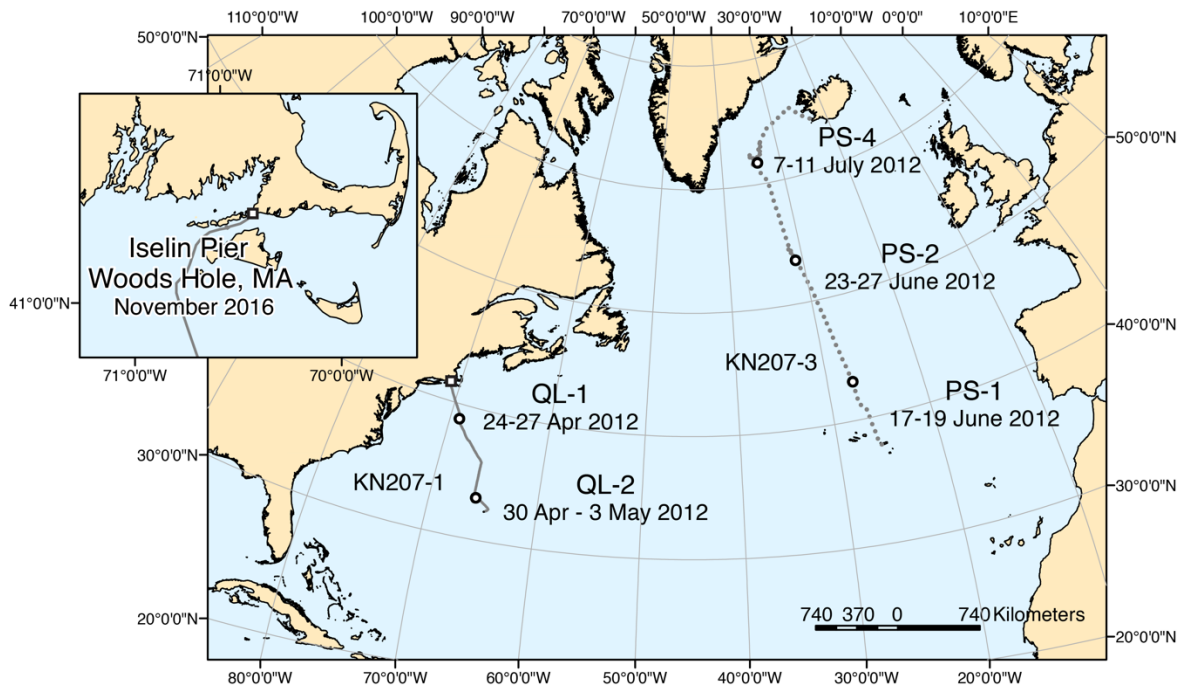
Fig. 2. Locations of PHORCYS deployments described in the text. Primary map: Unattended open-ocean deployments from a surface mooring were conducted using the PHORCYS prototype at 5 stations during two cruises aboard the *R/V Knorr*. Stations QL-1 and QL-2 were conducted during cruise KN207-1; PS-1, PS-2, and PS-3 were conducted during cruise KN207-3. Inset: Pierside deployments using the present PHORCYS model were conducted in November 2016 at the Iselin Marine Facility in Woods Hole, MA, USA.
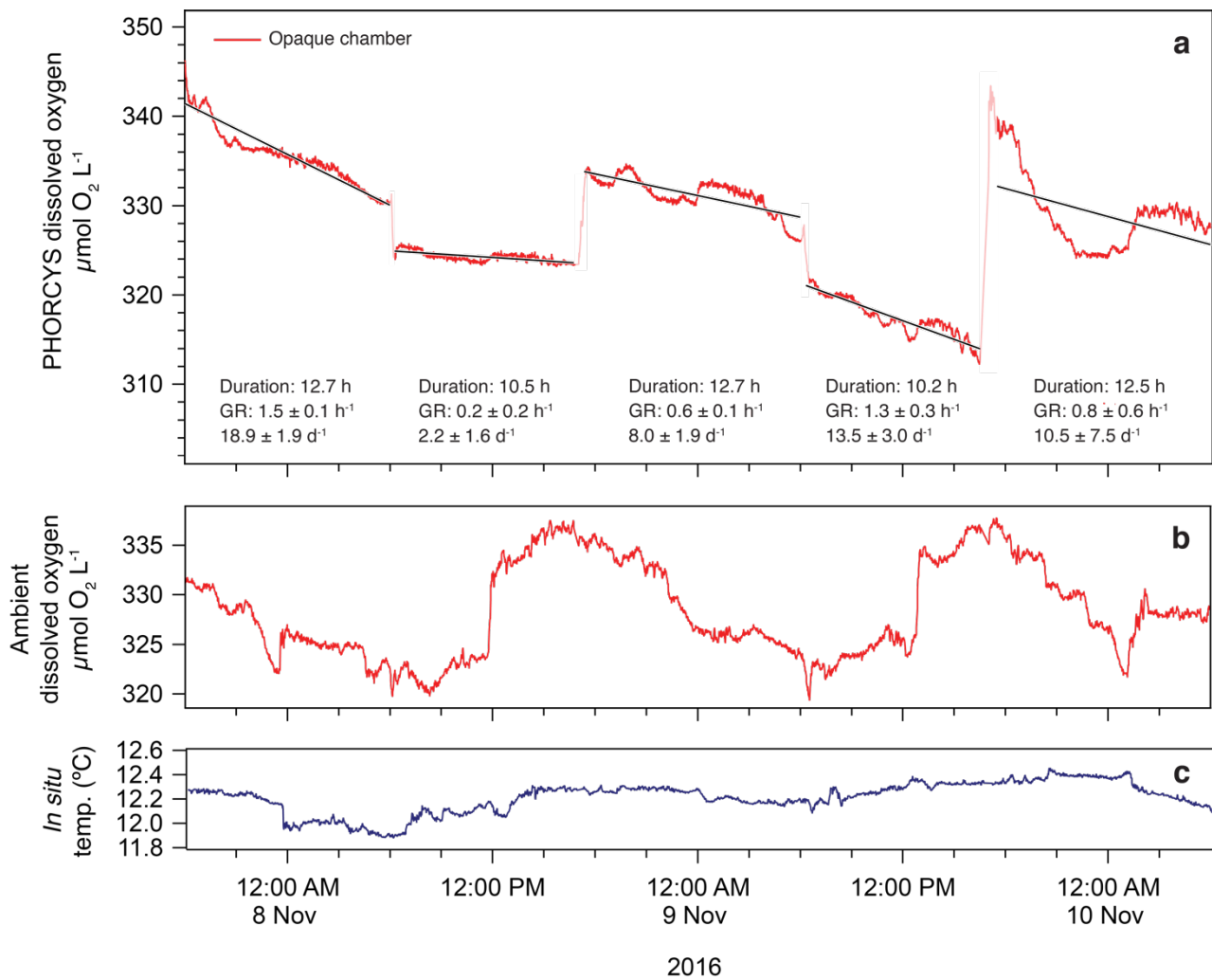
Fig. 3. Continuous, unattended observations of community respiration at the Iselin Pier in Woods Hole over a 3 d period in November 2016. (a) Record of dissolved oxygen concentration in the opaque PHORCYS chamber. The incubation periods from which estimates of GR were calculated are separated by 30 min, *in situ* flushing periods when the chamber was opened and closed to obtain a new water sample. Separate estimates of GR for each of the incubation periods (units of μmol O_2 L^{-1} d^{-1}) were obtained by linear least-squares regression, and are shown as solid traces superimposed over the instrument data; these are the Iselin Pier data reported in Tables 2 and A1. Uncertainties were determined using the effective degrees of freedom method described in the Appendix. (b) Ambient *in situ* dissolved oxygen concentration measured concurrently outside the PHORCYS chambers, reflecting tidal changes in water-mass properties. (c) Ambient *in situ* temperature data

29

602   recorded outside the PHORCYS chambers. An instrument malfunction during the deployment

603   prevented us from recovering data from the transparent PHORCYS chamber.
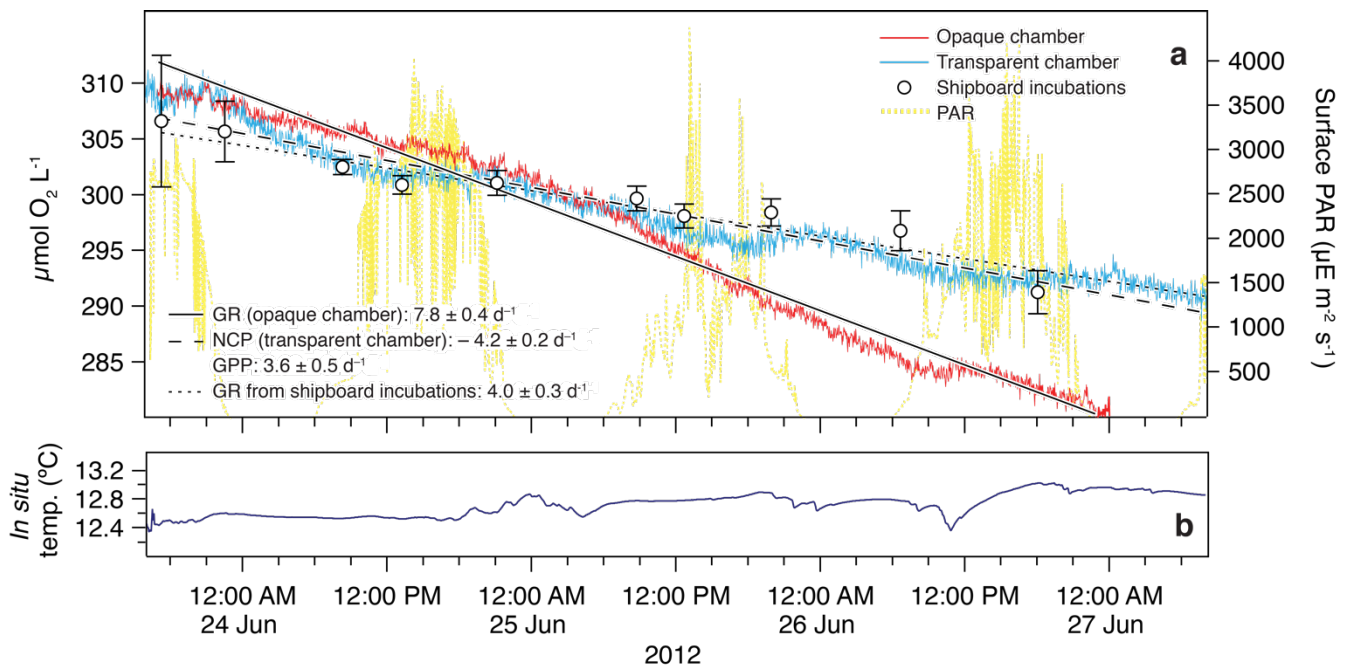
Fig. 4. Unattended observations of ecosystem metabolism made with the prototype PHORCYS instrument at station PS-2 (Fig. 2; Supplemental Table 1) during a sub-Arctic, open-ocean deployment aboard the R/V *Knorr*. A midsummer bloom of a calcifying phytoplankton species was in progress at the site (Collins et al., 2015) when these observations were made. (a) Estimates (in units of μmol O_2 L^{-1} d^{-1}) of gross community respiration (GR) and net community production (NCP) were obtained by linear least-squares regression, and are shown as traces (GR as solid trace; NCP as dashed trace) superimposed over the instrument data. The prototype instrument allowed for only a single incubation over the course of the deployment. GPP was calculated as the difference between GR and NCP based on Eq. 4 in the text. Uncertainties were determined using the effective degrees of freedom method described in the Appendix. Incident photosynthetically active radiation (PAR) was measured using shipboard sensors. Dissolved oxygen concentrations measured concurrently in dark shipboard incubations using optode sensor spots (5 replicates; error bars show ± SD) are superimposed as open circles. The respiration rate estimated from these incubations is shown as a dotted trace. (b) Diel warming of the surface layer is evident in *in situ* temperature data collected by the PHORCYS.
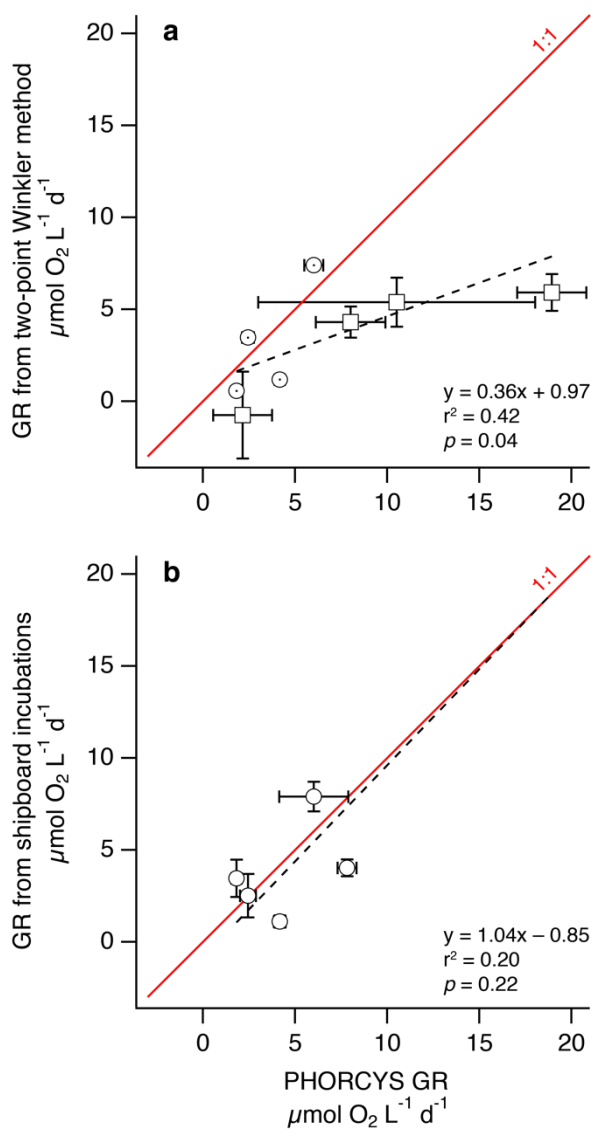
31

Fig. 5. Comparison of community respiration (GR) rate estimates from the PHORCYS (*x*-axis) with rates determined by (a) the two-point Winkler titration method and (b) a series of shipboard bottle incubations using optode sensor spots. Circles show data from the prototype instrument, while squares show data collected with the present PHORCYS model. A Type II (major axis) regression (dashed line) was fit to each set of paired observations using the lmodel2 package for R (Legendre, 2014). In (a), the regression model was fit to a single dataset consisting of both current and prototype model data. A red 1:1 line is superimposed in each panel for reference.

629 **Table 1.** Estimated surface area to volume ratios of PHORCYS chambers and standard BOD bottles.
630

Bottle or chamber type	Actual usable volume (mL)	Estimated internal surface area (cm^2)	Estimated surface area : volume ratio
PHORCYS chamber (prototype)	2610	1760	0.67
PHORCYS chamber (current model)	5680	2035	0.34
Typical 125 mL BOD bottle	149.2 ± 0.3	124.4 ± 5.0	0.83
Typical 300 mL BOD bottle	299.2 ± 0.4	229.1 ± 4.3	0.77

631
632 The average volumes and surface areas reported in this table for BOD bottles were determined from
633 independent measurements of the dimensions of 10 different bottles of each size; these were chosen
634 at random from the Woods Hole Oceanographic Institution inventory.

635   **Table 2.** Rates of community respiration measured in opaque bottles using the PHORCYS and two independent, traditional methods.

Deployment dates	Incubation period	Incubation duration (h)	Location[a]	PHORCYS model[b]	Community respiration (GR) (μmol O_2 L^{-1} d^{-1} ± uncertainty)		
					PHORCYS opaque bottle[c]	Shipboard incubations[d]	Two-point difference of Winkler titrations at t=0 and recovery[e]
24-27 Apr 2012	Entire deployment	71.6	QL-1	Prototype	1.8 ± 0.2	3.2 ± 0.7	0.6 ± 0.1
30 Apr - 3 May 2012	Entire deployment	65.4	QL-2	Prototype	4.2 ± 0.3	1.1 ± 0.2	1.2 ± 0.04
17-19 June 2012	Entire deployment	41.2	PS-1	Prototype	2.4 ± 0.3	3.4 ± 0.5	3.5 ± 0.2
23-27 June 2012	Entire deployment	77.4	PS-2	Prototype	7.8 ± 0.4	4.0 ± 0.3	—
7-11 July 2012	Entire deployment	94.0	PS-4	Prototype	6.0 ± 0.5	7.9 ± 0.6	7.4 ± 0.2
7-8 Nov 2016	17:15-06:00	12.7	Iselin Pier	Present model	18.9 ± 1.9	—	5.9 ± 1.0
8 Nov 2016	06:15-16:45	10.5	Iselin Pier	Present model	2.2 ± 1.6	—	−0.8 ± 2.4
8-9 Nov 2016	17:20-06:00	12.7	Iselin Pier	Present model	8.0 ± 1.9	—	4.3 ± 0.9
9-10 Nov 2016	17:30-06:00	12.5	Iselin Pier	Present model	10.5 ± 7.5	—	5.4 ± 1.3

636
637   [a] Cruise station or geographical location (Fig. 2); additional metadata for each station are provided in Supplemental Table 1
638   [a] See Fig. 1
639   [c] Uncertainty adjusted for effective degrees of freedom, as described in the Appendix
640   [d] Mean of ≥ 5 replicates; uncertainty derived from standard error of regression slope
641   [e] Mean of 3 replicates; uncertainty derived from standard error

642 **Table A1.** Comparison of methods for estimation of uncertainties in dissolved oxygen time series data.
643

Deployment dates	Location[a]	PHORCYS community respiration (GR) (μmol O_2 L^{-1} d^{-1})	No. obser-vations (N)	Incubation duration (h)	Est. integral time scale (h)	Effective degrees of freedom (N_{eff})	Estimated uncertainty (μmol O_2 L^{-1} d^{-1})		Method precision (est. uncertainty as percent of rate measurement)	
							Standard error of regression slope ($s_{\hat{\beta}_1}$)	Adjusted estimate $s_{\hat{\beta}_{1,adj}}$ based on N_{eff}	$s_{\hat{\beta}_1}$	$s_{\hat{\beta}_{1,adj}}$
24-27 Apr 2012	QL-1	1.8	2150	71.6	1.1	66.5	0.03	0.18	1.6 %	9.9 %
30 Apr - 3 May 2012	QL-2	4.2	1964	65.4	3.1	21.0	0.03	0.28	0.7 %	6.7 %
17-19 June 2012	PS-1	2.4	1238	41.2	0.5	76.4	0.08	0.32	3.3 %	13.1 %
23-27 June 2012	PS-2	7.8	2323	77.4	7.2	10.7	0.03	0.43	0.4 %	5.5 %
7-11 July 2012	PS-4	6.0	2820	94.0	1.9	49.8	0.07	0.52	1.2 %	8.6 %
7-8 Nov 2016	Iselin Pier	18.9	765	12.7	1.3	19.8	0.29	1.87	1.5 %	9.9 %
8 Nov 2016	Iselin Pier	2.2	627	10.5	1.2	17.0	0.25	1.60	11.6 %	74.4 %
8-9 Nov 2016	Iselin Pier	8.0	760	12.7	1.6	16.2	0.26	1.89	3.2 %	23.6 %
9-10 Nov 2016	Iselin Pier	10.5	750	12.5	2.9	8.7	0.71	7.51	6.7 %	71.4 %
Mean					2.3				3.4 %	24.8 %

644
645 [a] Cruise station or geographical location (Fig. 2); additional metadata for each station are provided in Supplemental Table 1
646
647
648

References

Anderson, L.A., and Sarmiento, J.L. 1994. Redfield ratios of remineralization determined by nutrient data-analysis. *Global Biogeochemical Cycles* 8, 65-80.

Aranguren-Gassis, M., Serret, P., Fernández, E., Herrera, J.L., Domínguez, J.F., Pérez, V., and Escanez, J. 2012. Balanced plankton net community metabolism in the oligotrophic North Atlantic subtropical gyre from Lagrangian observations. *Deep Sea Research Part I: Oceanographic Research Papers* 68, 116-122.

Belcher, A., Iversen, M., Giering, S., Riou, V., Henson, S.A., Berline, L., Guilloux, L. and Sanders, R. 2016a. Depth-resolved particle-associated microbial respiration in the northeast Atlantic. *Biogeosciences* 13, 4927-4943.

Belcher, A., Iversen, M., Manno, C., Henson, S.A., Tarling, G.A. and Sanders, R. 2016b. The role of particle associated microbes in remineralization of fecal pellets in the upper mesopelagic of the Scotia Sea, Antarctica. *Limnology and Oceanography* 61, 1049-1064.

Bender, M., Grande, K., Johnson, K., Marra, J., Williams, P.J., Sieburth, J., Pilson, M., Langdon, C., Hitchcock, G., Orchardo, J., Hunt, C., Donaghay, P., and Heinemann, K. 1987. A comparison of 4 methods for determining planktonic community production. *Limnology and Oceanography* 32, 1085-1098.

Bender, M., Orchardo, J., Dickson, M.-L., Barber, R., and Lindley, S. 1999. *In vitro* O_2 fluxes compared with ^{14}C production and other rate terms during the JGOFS Equatorial Pacific experiment. *Deep Sea Research Part I: Oceanographic Research Papers* 46, 637-654.

Boyd, P.W., McDonnell, A., Valdez, J., Lefevre, D., and Gall, M.P. 2015. RESPIRE: An *in situ* particle interceptor to conduct particle remineralization and microbial dynamics studies in the oceans' Twilight Zone. *Limnology and Oceanography: Methods* 13, 494-508.

Caffrey, J. 2004. Factors controlling net ecosystem metabolism in U.S. estuaries. *Estuaries and Coasts* 27, 90-101.

Calvo-Díaz, A., Díaz-Pérez, L., Suárez, L.Á., Morán, X.a.G., Teira, E., and Marañón, E. 2011. Decrease in the autotrophic-to-heterotrophic biomass ratio of picoplankton in oligotrophic marine waters due to bottle enclosure. *Applied and Environmental Microbiology* 77, 5739-5746.

Collins, J.R., Edwards, B.R., Thamatrakoln, K., Ossolinski, J.E., Ditullio, G.R., Bidle, K.D., Doney, S.C., and Van Mooy, B.A.S. 2015. The multiple fates of sinking particles in the North Atlantic Ocean. *Global Biogeochemical Cycles* 29, 1471-1494.

Collins, J.R., Raymond, P.A., Bohlen, W.F., and Howard-Strobel, M.M. 2013. Estimates of new and total productivity in Central Long Island Sound from *in situ* measurements of nitrate and dissolved oxygen. *Estuaries and Coasts* 36, 74–97.

Dang, H. and Lovell, C.R. 2016. Microbial surface colonization and biofilm development in marine environments. *Microbiol. Mol. Biol. Rev*. 80, 91-138.

686 Del Giorgio, P.A., and Williams, P.J. 2005. *Respiration in Aquatic Ecosystems.* Oxford, U.K.:
687 Oxford University Press.

688 Del Giorgio, P.A., and Pace, M.L. 2008. Relative independence of organic carbon transport and
689 processing in a large temperate river: The Hudson River as both pipe and reactor. *Limnol. Oceanogr.*
690 53, 185-197.

691 Delauney, L., Compère, C., and Lehaitre, M. 2010. Biofouling protection for marine environmental
692 sensors. Ocean Science 6, 503-511.

693 Denman, K.L., Brasseur, G., Chidthaisong, A., Ciais, P., Cox, P.M., Dickinson, R.E., Hauglustaine,
694 D., Heinze, C., Holland, E., Jacob, D., Lohmann, U., Ramachandran, S., Da Silva Dias, P.L., Wofsy,
695 S.C., and Zhang, X. 2007. "Couplings between changes in the climate system and biogeochemistry,"
696 in *Climate Change 2007: The Physical Science Basis. Contribution of Working Group I to the Fourth
697 Assessment Report of the Intergovernmental Panel on Climate Change,* eds. S. Solomon, D. Qin, M.
698 Manning, Z. Chen, M. Marquis, K.B. Averyt, T. M. & H.L. Miller. (Cambridge, U.K.: Cambridge
699 University Press), 89 p.

700 Duarte, C.M., Regaudie-De-Giroux, A., Arrieta, J.M., Delgado-Huertas, A., and Agustí, S. 2013. The
701 oligotrophic ocean is heterotrophic. *Annual Review of Marine Science* 5, 18.11–18.19.

702 Ducklow, H.W., and Doney, S.C. 2013. What is the metabolic state of the oligotrophic ocean? A
703 debate. *Annual Review of Marine Science* 5, 15.11–15.19.

704 Edwards, B.R., Reddy, C.M., Camilli, R., Carmichael, C.A., Longnecker, K., and Van Mooy, B.A.S.
705 2011. Rapid microbial respiration of oil from the Deepwater Horizon spill in offshore surface waters
706 of the Gulf of Mexico. *Environmental Research Letters* 6.

707 Emery, W.J., and Thomson, R.E. 2001. *Data Analysis Methods in Physical Oceanography.*
708 Amsterdam: Elsevier Science.

709 Figueroa, F.L., Mercado, J.M., Beardall, J., Neale, P.J., Montecino, V. and Kromkamp, J.C. 2014.
710 Introduction. *Aquatic Biology* 22, 1-4.

711 Fogg, G.E., and Calvario-Martinez, O. 1989. Effects of bottle size in determinations of primary
712 productivity by phytoplankton. *Hydrobiologia* 173, 89-94.

713 Fuchsman, C.A., Devol, A.H., Chase, Z., Reimers, C.E., and Hales, B. 2015. Benthic fluxes on the
714 Oregon shelf. *Estuarine, Coastal and Shelf Science* 163, Part B, 156-166.

715 Furnas, M.J. 2002. "Measuring the growth rates of phytoplankton in natural populations," in *Pelagic
716 Ecology Methodology,* ed. D.V.S. Rao. (Lisse: A. A. Balkema Publishers), 221-249.

717 Gaarder, T., and Gran, H.H. 1927. Investigations of the production of plankton in the Oslo Fjord.
718 *Rapports et Procès-Verbaux des Réunions du Conseil Permanent International pour l'Exploration de
719 la Mer* 42, 1-48.

720 Goldman, J.A.L., Kranz, S.A., Young, J.N., Tortell, P.D., Stanley, R.H.R., Bender, M.L., and Morel,
721 F.M.M. 2015. Gross and net production during the spring bloom along the Western Antarctic
722 Peninsula. *New Phytologist* 205, 182-191.

723   Guillemette, F., and del Giorgio, P.A. 2011. Reconstructing the various facets of dissolved organic
724   carbon bioavailability in freshwater ecosystems. *Limnol. Oceanogr.* 56, 734-748.

725   Guillemette, F., McCallister, S.L., and del Giorgio, P.A. 2013. Differentiating the degradation
726   dynamics of algal and terrestrial carbon within complex natural dissolved organic carbon in
727   temperate lakes. *Journal of Geophysical Research: Biogeosciences* 118, 963-973.

728   Hammond, D.E., Cummins, K.M., Mcmanus, J., Berelson, W.M., Smith, G., and Spagnoli, F. 2004.
729   Methods for measuring benthic nutrient flux on the California Margin: Comparing shipboard core
730   incubations to *in situ* lander results. *Limnology and Oceanography: Methods* 2, 146-159.

731   Karl, D.M., Dore, J.E., and Paul, J.H. 2001. "Microbial ecology at sea: Sampling, subsampling and
732   incubation considerations," in *Methods in Microbiology,* ed. J.H. Paul. (Waltham, MA, USA:
733   Academic Press), 13-39.

734   Kenner, R.A., and Ahmed, S.I. 1975. Measurements of electron transport activities in marine
735   phytoplankton. *Marine Biology* 33, 119-127.

736   Kim, S.-H., Choi, A., Jin Yang, E., Lee, S., and Hyun, J.-H. 2016. Low benthic respiration and
737   nutrient flux at the highly productive Amundsen Sea Polynya, Antarctica. *Deep Sea Research Part*
738   *II: Topical Studies in Oceanography* 123, 92-101.

739   Kjeldsen, P. 1993. Evaluation of gas diffusion through plastic materials used in experimental and
740   sampling equipment. *Water Research* 27, 121-131.

741   Klimant, I., Meyer, V., and Kühl, M. 1995. Fiber-optic oxygen microsensors, a new tool in aquatic
742   biology. *Limnology and Oceanography* 40, 1159-1165.

743   Knapp, G.P., Stalcup, M.C., and Stanley, R.J. 1989. "Dissolved oxygen measurements in sea water at
744   the Woods Hole Oceanographic Institution." Report WHOI-89-23. Woods Hole, MA: Woods Hole
745   Oceanographic Institution, 18 p.

746   Langdon, C., Marra, J., and Knudson, C. 1995. Measurements of net and gross O_2 production, dark
747   O_2 respiration, and ^{14}C assimilation at the Marine Light-Mixed Layers site (59°N, 21°W) in the
748   northeast Atlantic Ocean. *Journal of Geophysical Research: Oceans* 100, 6645-6653.

749   Lee, J.S., An, S.-U., Park, Y.-G., Kim, E., Kim, D., Kwon, J.N., Kang, D.-J., and Noh, J.-H. 2015.
750   Rates of total oxygen uptake of sediments and benthic nutrient fluxes measured using an *in situ*
751   autonomous benthic chamber in the sediment of the slope off the southwestern part of Ulleung Basin,
752   East Sea. *Ocean Science Journal* 50, 581-588.

753   Legendre, P. 2014. "lmodel2: Model II Regression." R package, version 1.7-2.

754   Manov, D.V., Chang, G.C., and Dickey, T.D. 2004. Methods for reducing biofouling of moored
755   optical sensors. Journal of Atmospheric and Oceanic Technology 21, 958-968.

756   Martens, C.S., Mendlovitz, H.P., Seim, H., Lapham, L., and D'Emidio, M. 2016. Sustained *in situ*
757   measurements of dissolved oxygen, methane and water transport processes in the benthic boundary
758   layer at MC118, northern Gulf of Mexico. *Deep Sea Research Part II: Topical Studies in*
759   *Oceanography* 129, 41-52.

760   McDonnell, A.M.P., Boyd, P.W., and Buesseler, K.O. 2015. Effects of sinking velocities and
761   microbial respiration rates on the attenuation of particulate carbon fluxes through the mesopelagic
762   zone. *Global Biogeochemical Cycles* 29, 2014GB004935.

763   Moore, C., Barnard, A., Fietzek, P., Lewis, M.R., Sosik, H.M., White, S., and Zielinski, O. 2009.
764   Optical tools for ocean monitoring and research. *Ocean Science* 5, 661-684.

765   Nicholson, D.P., Wilson, S.T., Doney, S.C., and Karl, D.M. 2015. Quantifying subtropical North
766   Pacific gyre mixed layer primary productivity from Seaglider observations of diel oxygen cycles.
767   *Geophysical Research Letters* 42, 4032-4039.

768   Porter, J.H., Nagy, E., Kratz, T.K., Hanson, P., Collins, S.L., and Arzberger, P. 2009. New eyes on
769   the world: Advanced sensors for ecology. *Bioscience* 59, 385-397.

770   Pratt, D.M. and Berkson, H. 1959. Two sources of error in the oxygen light and dark bottle method.
771   *Limnology and Oceanography* 4, 328-334.

772   Prien, R.D. 2007. The future of chemical *in situ* sensors. *Marine Chemistry* 107, 422-432.

773   Quay, P.D., Peacock, C., Björkman, K., and Karl, D.M. 2010. Measuring primary production rates in
774   the ocean: Enigmatic results between incubation and non-incubation methods at Station ALOHA.
775   *Global Biogeochem. Cycles* 24, GB3014.

776   Redfield, A.C. 1934. "On the proportions of organic derivatives in sea water and their relation to the
777   composition of plankton," in *James Johnstone Memorial Volume,* ed. R.J. Daniel. University Press of
778   Liverpool), 176-192.

779   Regaudie-De-Gioux, A., Lasternas, S., Agustí, S., and Duarte, C.M. 2014. Comparing marine
780   primary production estimates through different methods and development of conversion equations.
781   *Frontiers in Marine Science* 1.

782   Reinthaler, T., Van Aken, H.M., and Herndl, G.J. 2010. Major contribution of autotrophy to
783   microbial carbon cycling in the deep North Atlantic's interior. *Deep-Sea Research Part II-Topical*
784   *Studies in Oceanography* 57, 1572-1580.

785   Riser, S.C., and Johnson, K.S. 2008. Net production of oxygen in the subtropical ocean. *Nature* 451,
786   323-U325.

787   Robert, A. 2012. Mineralisation *in situ* de la matière organique le long de la colonne d'eau:
788   Application sur une station eulerienne. Dissertation. Marseille: Université d'Aix-Marseille.

789   Robinson, C., and Williams, P.J. 2005. "Respiration and its measurement in surface marine waters,"
790   in *Respiration in Aquatic Ecosystems,* eds. P. Del Giorgio & P.J. Williams. (New York: Oxford
791   University Press).

792   Robinson, C., Tilstone, G.H., Rees, A.P., Smyth, T.J., Fishwick, J.R., Tarran, G.A., Luz, B., Barkan,
793   E., and David, E. 2009. Comparison of *in vitro* and *in situ* plankton production determinations.
794   *Aquatic Microbial Ecology* 54, 13-34.

795 Salta, M., Wharton, J.A., Blache, Y., Stokes, K.R. and Briand, J.-F. 2013. Marine biofilms on
796 artificial surfaces: structure and dynamics. *Environ. Microbiol*. 15, 2879-2893.

797 Spanjers, H., Olsson, G., and Klapwijk, A. 1994. Determining short-term biochemical oxygen
798 demand and respiration rate in an aeration tank by using respirometry and estimation. *Water*
799 *Research* 28, 1571-1583.

800 Staehr, P.A., Testa, J.M., Kemp, W.M., Cole, J.J., Sand-Jensen, K., and Smith, S.V. 2012. The
801 metabolism of aquatic ecosystems: history, applications, and future challenges. *Aquatic Sciences* 74,
802 15-29.

803 Steeman Nielsen, E. 1952. The use of radioactive carbon (^{14}C) for measuring organic production in
804 the sea. *Journal du Conseil - Conseil International pour l'Exploration de la Mer* 18, 117-140.

805 Stumm, W., and Morgan, J.J. 2013. *Aquatic Chemistry: Chemical Equilibria and Rates in Natural*
806 *Waters*. New York: Wiley.

807 Suter, E.A., Scranton, M.I., Chow, S., Stinton, D., Medina Faull, L., and Taylor, G.T. 2016. Niskin
808 bottle sample collection aliases microbial community composition and biogeochemical interpretation.
809 *Limnology and Oceanography*. doi: 10.1002/lno.10447

810 Talley, L.D., Pickard, G.L., Emery, W.J., and Swift, J.H. 2011. "Data analysis concepts and
811 observational methods," in *Descriptive Physical Oceanography*. 6th ed (Boston: Academic Press),
812 147-186.

813 Tamburini, C., Boutrif, M., Garel, M., Colwell, R.R., and Deming, J.W. 2013. Prokaryotic responses
814 to hydrostatic pressure in the ocean – a review. *Environmental Microbiology* 15, 1262-1274.

815 Taylor, C.D., and Doherty, K.W. 1990. Submersible Incubation Device (SID), autonomous
816 instrumentation for the *in situ* measurement of primary production and other microbial rate processes.
817 *Deep-Sea Research Part A-Oceanographic Research Papers* 37, 343-358.

818 Taylor, C.D., Howes, B.L., and Doherty, K.W. 1993. Automated instrumentation for time-series
819 measurement of primary production and nutrient status in production platform-accessible
820 environments. *Marine Technology Society Journal* 27, s32-44.

821 Tengberg, A., Hovdenes, J., Andersson, H.J., Brocandel, O., Diaz, R., Hebert, D., Arnerich, T.,
822 Huber, C., Körtzinger, A., Khripounoff, A., Rey, F., Rönning, C., Schimanski, J., Sommer, S., and
823 Stangelmayer, A. 2006. Evaluation of a lifetime-based optode to measure oxygen in aquatic systems.
824 *Limnology and Oceanography: Methods* 4, 7-17.

825 Venrick, E.L., Beers, J.R., and Heinbokel, J.F. 1977. Possible consequences of containing
826 microplankton for physiological rate measurements. *Journal of Experimental Marine Biology and*
827 *Ecology* 26, 55-76.

828 Volkmar, E.C., and Dahlgren, R.A. 2006. Biological oxygen demand dynamics in the Lower San
829 Joaquin River, California. *Environmental Science & Technology* 40, 5653-5660.

830 Wang, Z.A., Sonnichsen, F.N., Bradley, A.M., Hoering, K.A., Lanagan, T.M., Chu, S.N., Hammar,
831 T.R., and Camilli, R. 2015. *In situ* sensor technology for simultaneous spectrophotometric

832   measurements of seawater total dissolved inorganic carbon and pH. *Environmental Science &*
833   *Technology* 49, 4441-4449.

834   Warkentin, M., Freese, H.M., Karsten, U., and Schumann, R. 2007. New and fast method to quantify
835   respiration rates of bacterial and plankton communities in freshwater ecosystems by using optical
836   oxygen sensor spots. *Applied and Environmental Microbiology* 73, 6722-6729.

837   Wikner, J., Panigrahi, S., Nydahl, A., Lundberg, E., Båmstedt, U., and Tengberg, A. 2013. Precise
838   continuous measurements of pelagic respiration in coastal waters with Oxygen Optodes. *Limnology*
839   *and Oceanography: Methods* 11, 1-15

840   Williams, P.J. 1998. The balance of plankton respiration and photosynthesis in the open oceans.
841   *Nature* 394, 55-57.

842   Williams, P.J., Quay, P.D., Westberry, T.K., and Behrenfeld, M.J. 2013. The oligotrophic ocean is
843   autotrophic. *Annual Review of Marine Science* 5, 16.11-16.15.

844   Winkler, L.W. 1888. Die Bestimmung des im Wasser gelosten Sauerstoffes. *Ber. Dtsch. Chem. Ges.*
845   *Berlin* 21, 2843-2846.

846   Yvon-Durocher, G., Caffrey, J.M., Cescatti, A., Dossena, M., Giorgio, P.D., Gasol, J.M., Montoya,
847   J.M., Pumpanen, J., Staehr, P.A., Trimmer, M., Woodward, G., and Allen, A.P. 2012. Reconciling
848   the temperature dependence of respiration across timescales and ecosystem types. *Nature* 487, 472-
849   476.